

CERN-TH/97-91  
 CPT-97/P3480  
 hep-ph/9712417

# Dispersive Bounds on the Shape of $\bar{B} \rightarrow D^{(*)} \ell \bar{\nu}$ Form Factors

Irinel Caprini

*Institute of Atomic Physics, Bucharest, POB MG-6, Romania*

Laurent Lellouch<sup>\*)</sup> and Matthias Neubert

*Theory Division, CERN, CH-1211 Geneva 23, Switzerland*

## Abstract

Dispersive constraints on the shape of the form factors which describe the exclusive decays  $\bar{B} \rightarrow D^{(*)} \ell \bar{\nu}$  are derived by fully exploiting spin symmetry in the ground-state doublet of heavy-light mesons. The analysis includes all twenty  $\bar{B}^{(*)} \rightarrow D^{(*)}$  semileptonic form factors. Heavy-quark symmetry, with both short-distance and  $1/m_Q$  corrections included, is used to provide relations between the form factors near zero recoil. Simple one-parameter functions are derived, which describe the form factors in the semileptonic region with an accuracy of better than 2%. The implications of our results for the determination of  $|V_{cb}|$  are discussed.

(Submitted to Nuclear Physics B)

CERN-TH/97-91  
 December 1997

<sup>\*)</sup> On leave from: Centre de Physique Théorique, Case 907, CNRS Luminy, F-13288 Marseille Cedex 9, France (UPR7061).

# 1 Introduction

The differential rates for the exclusive semileptonic decays  $\bar{B} \rightarrow D^{(*)} \ell \bar{\nu}$  are given by [1]

$$\begin{aligned} \frac{d\Gamma(\bar{B} \rightarrow D^* \ell \bar{\nu})}{dw} &= \frac{G_F^2 |V_{cb}|^2}{48\pi^3} (m_B - m_{D^*})^2 m_{D^*}^3 \sqrt{w^2 - 1} (w + 1)^2 \\ &\quad \times \left[ 1 + \frac{4w}{w + 1} \frac{m_B^2 - 2w m_B m_{D^*} + m_{D^*}^2}{(m_B - m_{D^*})^2} \right] |\mathcal{F}(w)|^2, \\ \frac{d\Gamma(\bar{B} \rightarrow D \ell \bar{\nu})}{dw} &= \frac{G_F^2 |V_{cb}|^2}{48\pi^3} (m_B + m_D)^2 m_D^3 (w^2 - 1)^{3/2} |V_1(w)|^2, \end{aligned} \quad (1)$$

where  $\mathcal{F}(w)$  and  $V_1(w)$  are hadronic form factors, and  $w = v_B \cdot v_{D^{(*)}}$  is the product of the velocities of the initial and final mesons. In the heavy-quark limit,  $\mathcal{F}(w)$  and  $V_1(w)$  coincide with the Isgur–Wise function  $\xi(w)$ , which describes the long-distance physics associated with the light degrees of freedom in the heavy mesons [2]. This function is normalized to unity at zero recoil, corresponding to  $w = 1$ . Corrections to this limit can be calculated using the heavy-quark effective theory [3], and are suppressed by powers of  $\alpha_s(m_Q)$  or  $\Lambda_{\text{QCD}}/m_Q$ , where we use  $m_Q$  generically for  $m_b$  or  $m_c$ . Detailed calculations of these corrections lead to  $\mathcal{F}(1) = 0.91 \pm 0.03$  [1], [4]–[7] and  $V_1(1) = 0.98 \pm 0.07$  [8], so that an accurate determination of  $|V_{cb}|$  can be obtained by extrapolating the differential decay rates to  $w = 1$ . To reduce the uncertainties associated with this extrapolation, constraints on the shape of the form factors are highly desirable. A suitable framework to derive such constraints is provided by a dispersion technique proposed some time ago [9]–[12], and has been applied to heavy-meson form factors more recently [13]–[20]. This method is based on first principles: the analyticity properties of two-point functions of local currents and the positivity of the corresponding spectral functions. Analyticity relates integrals of the hadronic spectral functions to the behavior of QCD two-point functions in the deep Euclidean region via dispersion relations. Positivity guarantees that the contributions of the states of interest to the spectral functions are bounded above. The constraints on the relevant form factors, given their analyticity properties, then follow from these bounds.

Following Refs. [18, 20], we generalize this method to fully exploit spin symmetry in the doublets of the ground-state  $B^{(*)}$  and  $D^{(*)}$  mesons. By taking into account all contributions related by heavy-quark symmetry, this generalization increases the constraining power of the method considerably. We investigate all spin–parity channels ( $J^P = 0^+, 0^-, 1^-$  and  $1^+$ ) relevant for  $\bar{B}^{(*)} \rightarrow D^{(*)}$  transitions. This gives us four inequalities and thus four allowed domains for the parameters which describe the form factors of interest. The optimal constraints are obtained by taking the intersection of these domains. Although these different channels were also investigated recently by the authors of Ref. [20], we bring a number of improvements to their analysis and exploit the dispersive techniques with a somewhat different emphasis. First, we include the contributions of the  $B_c$  poles to the relevant polarization functions. Since these contributions are positive, they reduce

the domain available to the contributions of the  $B^{(*)}D^{(*)}$  states and therefore increase the constraints on the corresponding form factors. As a second improvement, we include the short-distance and  $1/m_Q$  corrections to the heavy-quark limit in the relations between form factors, thereby eliminating the leading uncertainties in these relations. We further discuss the role of remaining uncertainties and show how their inclusion is necessary to avoid overinterpreting the results of the dispersive method. In addition, instead of requiring rather complicated kinematical functions and the knowledge of the singularity structure of individual form factors, we introduce single-parameter descriptions that are simple, low-order power-series expansions in kinematical variables, and accurate to 2% over the full semileptonic domain. Thus, these parametrizations will be very useful for reducing the uncertainty in the extraction of  $|V_{cb}|$  from experimental data.

The paper is organized as follows. In the next section, we present the derivation of the unitarity inequalities, which are the basis of the dispersive bounds on form factors discussed in Section 3. In Sections 4 and 5, we derive model-independent bounds on the heavy-meson form factors using expansions in different kinematical variables. We present a new method for including corrections to the heavy-quark limit, which fully takes into account the uncertainties in their calculation. We find that these uncertainties have a significant effect on the bounds and, ultimately, limit the accuracy of the dispersive approach. We also derive simple, one-parameter descriptions of the form factors in the semileptonic region. The phenomenological consequences of our results are discussed in Section 6, where the reader not interested in the technical details of our work can find a summary of our parametrizations for the  $\bar{B} \rightarrow D^{(*)}\ell\bar{\nu}$  form factors. Our conclusions are given in Section 7. The paper also comprises an Appendix, where we give the definitions of form factors and details of our calculations.

## 2 Dispersion relations and unitarity inequalities

We start with the vacuum polarization tensor

$$\begin{aligned}\Pi^{\mu\nu}(q) &= i \int d^4x e^{iq \cdot x} \langle 0 | T\{V^\mu(x), V^{\dagger\nu}(0)\} | 0 \rangle \\ &= (q^\mu q^\nu - g^{\mu\nu} q^2) \Pi_{1-}(q^2) + q^\mu q^\nu \Pi_{0+}(q^2),\end{aligned}\tag{2}$$

and a similar expression for the correlator of two axial currents with invariant functions  $\Pi_{1+}$  and  $\Pi_{0-}$ , where the subscripts indicate the spin-parity quantum numbers of the intermediate states contributing in the various channels. The invariant functions satisfy subtracted dispersion relations, which we write as ( $Q^2 = -q^2$ )

$$\begin{aligned}\chi_{0\pm}(Q^2) &= \left(-\frac{\partial}{\partial Q^2}\right) [-Q^2 \Pi_{0\pm}(Q^2)] = \frac{1}{\pi} \int_0^\infty dt \frac{t \operatorname{Im} \Pi_{0\pm}(t)}{(t + Q^2)^2}, \\ \chi_{1\pm}(Q^2) &= \frac{1}{2} \left(-\frac{\partial}{\partial Q^2}\right)^2 [-Q^2 \Pi_{1\pm}(Q^2)] = \frac{1}{\pi} \int_0^\infty dt \frac{t \operatorname{Im} \Pi_{1\pm}(t)}{(t + Q^2)^3}.\end{aligned}\tag{3}$$

In the Euclidean region, where  $Q^2 > 0$ , these functions can be calculated in QCD using the operator product expansion. On the other hand, the spectral functions  $\text{Im}\Pi_{0\pm}(t)$  and  $\text{Im}\Pi_{1\pm}(t)$  are given by unitarity relations. In the case of the vector correlator, we have

$$\begin{aligned} & (q^\mu q^\nu - g^{\mu\nu} q^2) \text{Im}\Pi_{1-}(q^2 + i\epsilon) + q^\mu q^\nu \text{Im}\Pi_{0+}(q^2 + i\epsilon) \\ &= \frac{1}{2} \sum_{\Gamma} d\rho_{\Gamma} (2\pi)^4 \delta^{(4)}(p_{\Gamma} - q) \langle 0 | V^{\mu}(0) | \Gamma \rangle \langle \Gamma | V^{\dagger\nu}(0) | 0 \rangle, \end{aligned} \quad (4)$$

and a similar relation holds for the axial correlator. The spectral functions, which are sums of positive terms, are bounded below by the contributions of the two-particle states  $|BD\rangle$ ,  $|BD^*\rangle$ ,  $|B^*D\rangle$ , and  $|B^*D^*\rangle$ , which are related through crossing symmetry to the matrix elements relevant for semileptonic decays. Combining this lower bound with the QCD result for the correlators, we derive constraints on the form factors in the semileptonic region. These constraints are further improved by using heavy-quark symmetry to relate the matrix elements associated with these different contributions. Note that, when extending the number of hadron states in the unitarity sum, there is, in principle, a danger of double counting if particles which decay via strong interactions are included. In our case,  $D^*$  accounts partially for the two-particle state  $D\pi$ , which therefore must not be included separately. ( $B^*$  is stable with respect to strong decays, since  $m_{B^*} < m_B + m_{\pi}$ .)

To further increase the constraining power of the dispersive method, we take into account the single-particle contributions of the first two vector  $B_c^*$  and pseudoscalar  $B_c$  mesons.<sup>1</sup> These contributions are determined in terms of the masses and leptonic decay constants of these states, whose values can be calculated rather accurately using quark models. In Table 1, we collect the masses and decay constants of all  $B_c$  mesons below the threshold for  $B^*D^*$  production, as predicted by the model of Ref. [21]. Note that the scalar and axial states, as well as some of the vector and pseudoscalar states, have non-vanishing orbital angular momentum and therefore vanishing decay constants. Although this conclusion is strictly only valid in the context of quark models, we expect orbitally excited states to have much smaller decay constants than S-wave states, and take the conservative approach of neglecting their contributions to the various spectral functions.

Inserting these one- and two-particle states into the unitarity sums, and combining the resulting bounds with the dispersion relations of (3), we find

$$\sum_{j=1,2,3} \int_{-\infty}^{-1} dw (w^2 - 1)^{1/2} \left( \frac{w+1}{2} \right)^2 (1 + \delta_{j2}) \frac{(\beta_j^2 - 1) |S_j(w)|^2}{\left( \beta_j^2 - \frac{w+1}{2} \right)^4} < \frac{64\pi^2}{n_f} \chi_{0+}(0),$$

---

<sup>1</sup>We do not include more massive resonances, because they lie above the  $BD$  threshold and may lead to double counting.

Table 1: *Masses (in GeV) and decay constants (in MeV) of the lowest-lying  $B_c$  states [21]*

$J^P$	$0^+$	$1^-$		$0^-$		$1^+$
$n$	$M_n$	$M_n$	$f_n$	$M_n$	$f_n$	$M_n$
1	6.700	6.337	497	6.264	500	6.730
2	7.108	6.899	369	6.856	370	6.736
3		7.012		7.244		7.135
4		7.280	327			7.142

$$\begin{aligned}
& \sum_{j=1,2,3} \int_{-\infty}^{-1} dw (w^2 - 1)^{3/2} (1 + \delta_{j2}) \frac{\beta_j^2 |V_j(w)|^2}{\left(\beta_j^2 - \frac{w+1}{2}\right)^5} \\
& + \sum_{j=4,5,6,7} \int_{-\infty}^{-1} dw (w^2 - 1)^{3/2} \frac{2|V_j(w)|^2}{\left(\beta_j^2 - \frac{w+1}{2}\right)^5} < \frac{3072\pi^2}{n_f} m_{B^*} m_{D^*} \tilde{\chi}_{1^-}(0), \\
& \sum_{j=1,2,3} \int_{-\infty}^{-1} dw (w^2 - 1)^{3/2} (1 + \delta_{j3}) \frac{\beta_j^2 |P_j(w)|^2}{\left(\beta_j^2 - \frac{w+1}{2}\right)^4} < \frac{256\pi^2}{n_f} \tilde{\chi}_{0^-}(0), \\
& \sum_{j=1,2,3,4} \int_{-\infty}^{-1} dw (w^2 - 1)^{1/2} \left(\frac{w+1}{2}\right)^2 \frac{2|A_j(w)|^2}{\left(\beta_j^2 - \frac{w+1}{2}\right)^4} \\
& + \sum_{j=5,6,7} \int_{-\infty}^{-1} dw (w^2 - 1)^{1/2} \left(\frac{w+1}{2}\right)^2 (1 + \delta_{j7}) \frac{(\beta_j^2 - 1)|A_j(w)|^2}{\left(\beta_j^2 - \frac{w+1}{2}\right)^5} \\
& < \frac{768\pi^2}{n_f} m_{B^*} m_{D^*} \chi_{1^+}(0), \tag{5}
\end{aligned}$$

where we have set  $Q^2 = 0$  for simplicity. In principle, the inequalities could be strengthened by using negative values of  $Q^2$ , which however must be sufficiently far away from threshold in order for the operator product expansion to be well defined. However, in Ref. [19] it was found that this would improve the bounds only slightly. Therefore, we shall not consider this possibility any further.

In terms of the kinematical variable  $w$  entering the unitarity inequalities, the momentum transfer  $t = q^2$  appearing in (2) and (3) is given by

$$t = q^2 = m_{B^{(*)}}^2 + m_{D^{(*)}}^2 - 2m_{B^{(*)}}m_{D^{(*)}}w. \tag{6}$$

We work with  $w$  instead of  $t$  because it is the natural variable for implementing heavy-quark symmetry, and because the various  $B^{(*)}D^{(*)}$  thresholds, which occur at different values of  $t$ , all occur at the same value  $w = -1$ , enabling a unified treatment of all form factors. The form factors  $V_i$ ,  $S_i$ ,  $A_i$  and  $P_i$ , which appear in (5), are linear combinations of the traditional heavy-quark basis form factors chosen (i) to reduce to the Isgur–Wise function in the heavy-quark limit, (ii) to have definite spin–parity quantum numbers ( $1^-$ ,  $0^+$ ,  $1^+$  and  $0^-$ , respectively), and (iii) to reduce the unitarity relations to sums of squares. The definitions of these form factors are given in the Appendix. The factor of  $n_f$  appears in (5) because  $SU(n_f)$  light-flavour multiplets of heavy-meson states contribute with the same weight to the unitarity sums. To be conservative, we take  $n_f = 2.5$  to account for the breaking of  $SU(3)$  flavour symmetry due to the strange-quark mass. For each  $\bar{B}^{(*)} \rightarrow D^{(*)}$  transition form factor, we define a quantity

$$\beta_j = \frac{m_{B^{(*)}} + m_{D^{(*)}}}{2\sqrt{m_{B^{(*)}}m_{D^{(*)}}}}, \quad (7)$$

where it is understood that the appropriate masses are used. Moreover, we use the notation

$$\begin{aligned} \tilde{\chi}_{1-}(0) &= \chi_{1-}(0) - \sum_{n=1,2} \frac{f_n^2(B_c^*)}{M_n^4(B_c^*)}, \\ \tilde{\chi}_{0-}(0) &= \chi_{0-}(0) - \sum_{n=1,2} \frac{f_n^2(B_c)}{M_n^2(B_c)}, \end{aligned} \quad (8)$$

and thus include the contributions of the first two vector  $B_c^*$  and scalar  $B_c$  mesons to the polarization functions.

For the vector correlator, the leading terms in the operator product expansion of the vacuum polarization functions are given by

$$\begin{aligned} \chi_{0+}(Q^2) &= \frac{3}{4\pi^2} \int_0^1 dx x(1-x) \frac{xm_b^2 + (1-x)m_c^2 - m_b m_c}{xm_b^2 + (1-x)m_c^2 + x(1-x)Q^2}, \\ \chi_{1-}(Q^2) &= \frac{3}{8\pi^2} \int_0^1 dx x^2(1-x)^2 \frac{3xm_b^2 + 3(1-x)m_c^2 + m_b m_c + 2x(1-x)Q^2}{[xm_b^2 + (1-x)m_c^2 + x(1-x)Q^2]^2}, \end{aligned} \quad (9)$$

where  $m_b$  and  $m_c$  are the heavy-quark masses. The functions  $\chi_{0-}$  and  $\chi_{1+}$  for the axial correlator are obtained from these expressions by the replacement  $m_c \rightarrow -m_c$ . Evaluating these results at  $Q^2 = 0$ , and using  $z = m_c/m_b = 0.29 \pm 0.03$  for the ratio of the heavy-quark pole masses, we obtain:  $\chi_{0+}(0) = 4.40_{+0.58}^{-0.52} \times 10^{-3}$ ,  $m_b^2 \chi_{1-}(0) = 9.92_{+0.17}^{-0.19} \times 10^{-3}$ ,  $\chi_{0-}(0) = 2.09_{-0.06}^{+0.05} \times 10^{-2}$ , and  $m_b^2 \chi_{1+}(0) = 6.06_{+0.28}^{-0.27} \times 10^{-3}$ . For the spin-1 channels, we use the value  $m_b = (4.8 \pm 0.2) \text{ GeV}$ . The  $O(\alpha_s)$  corrections, which have been calculated in Refs. [22]–[24], enhance these results by 29%, 31%, 14%, and 29%, respectively, where we use  $\alpha_s = \alpha_s(m_b) = 0.22$ . The leading nonperturbative

corrections, proportional to the quark and gluon condensates, are very small and can be neglected [23, 25]. With these parameters, we obtain

$$\begin{aligned}
\chi_{0+}(0) &= (5.69 \pm 0.71) \times 10^{-3}, \\
m_{B^*} m_{D^*} \tilde{\chi}_{1-}(0) &= (3.73 \pm 0.51) \times 10^{-3}, \\
\tilde{\chi}_{0-}(0) &= (1.46 \pm 0.06) \times 10^{-2}, \\
m_{B^*} m_{D^*} \chi_{1+}(0) &= (3.63 \pm 0.34) \times 10^{-3}.
\end{aligned} \tag{10}$$

In the  $1^-$  and  $0^-$  channels, we have subtracted the pole contributions from the two lowest  $B_c$  and  $B_c^*$  mesons using the values of the decay constants shown in Table 1. In the evaluation of the inequalities (5), we choose to relate all form factors to the reference form factor  $V_1(w)$ , which governs the  $\bar{B} \rightarrow D \ell \bar{\nu}$  decay rate in (1), and whose normalization at zero recoil is  $V_1(1) = 0.98 \pm 0.07$  [8]. Then, what enters the inequalities (5) are the products of the correlation functions divided by  $n_f V_1^2(1)$ . The unitarity bounds become weaker the larger the values of the correlation functions and the smaller the value of  $V_1(1)$ . Therefore, we simultaneously lower the value of the form factor and increase the central values in (10) by one standard deviation. This leads to the conservative upper bounds

$$\begin{aligned}
\frac{\chi_{0+}(0)}{n_f V_1^2(1)} &< 3.1 \times 10^{-3}, & m_{B^*} m_{D^*} \frac{\tilde{\chi}_{1-}(0)}{n_f V_1^2(1)} &< 2.0 \times 10^{-3}, \\
\frac{\tilde{\chi}_{0-}(0)}{n_f V_1^2(1)} &< 7.3 \times 10^{-3}, & m_{B^*} m_{D^*} \frac{\chi_{1+}(0)}{n_f V_1^2(1)} &< 1.9 \times 10^{-3},
\end{aligned} \tag{11}$$

which we use in our analysis.

### 3 Model-independent bounds on form factors

The four inequalities in (5) can be used to derive bounds on the corresponding form factors in the semileptonic domain. The problem is brought into a canonical form by performing a conformal mapping  $w \rightarrow z(w, a)$ , which transforms the cut  $w$  plane onto the interior of the unit disc  $|z| < 1$ , such that the integrals in (5) become integrals around the unit circle  $z = e^{i\theta}$ . This is achieved by defining

$$z(w, a) = \frac{\sqrt{w+1} - \sqrt{2}a}{\sqrt{w+1} + \sqrt{2}a}; \quad a > 0, \tag{12}$$

which maps the branch point  $w = -1$  onto  $z = -1$ . The choice of the real parameter  $a$  will be discussed later.

As explained in previous works [12]–[18], one further introduces a set of “outer” functions  $\phi_j(z)$ , i.e. functions without zeros nor singularities inside the unit disc, such

that the unitarity inequalities take the form

$$\frac{1}{2\pi} \int_0^{2\pi} d\theta \sum_j \left| \phi_j(e^{i\theta}) F_j(w) \right|^2 \leq 1, \quad (13)$$

where it is implied that  $w$  is expressed in terms of  $z = e^{i\theta}$  by means of (12). Here  $F_j$  is one of the scalar, pseudoscalar, vector or axial-vector form factors, and  $j$  runs over the set of form factors in a given spin-parity channel. Along the unit circle, the modulus squared of the outer functions are equal to the weights in front of the corresponding form factors in (5), multiplied by the modulus of the Jacobian of the conformal transformation (12). The calculation of these functions is straightforward. The weight functions appearing in the inequalities are of the generic form

$$N (w^2 - 1)^{3/2-n} \left( \frac{w+1}{2} \right)^{2n} \left( \beta^2 - \frac{w+1}{2} \right)^{-m}, \quad (14)$$

where  $N$  is a constant. The corresponding outer functions are given by

$$\begin{aligned} \phi(z) = & \sqrt{2\pi N} \frac{4^{2-n} a^4}{(\beta+a)^m} \left( \frac{1+a}{2a} \right)^{3/2-n} (1+z)^{n+2} (1-z)^{m-9/2} \\ & \times \left( 1 - z \frac{\beta-a}{\beta+a} \right)^{-m} \left( 1 - z \frac{1-a}{1+a} \right)^{3/2-n}. \end{aligned} \quad (15)$$

In deriving bounds on the values or derivatives of the form factors inside the unit disc, one must account for the effects of singularities located below the physical thresholds. For simplicity, we discuss the singularity structure in terms of the momentum transfer  $q^2$  given in (6). For the form factors of interest, the thresholds occur at the values of  $\sqrt{q^2}$  at which the relevant  $B^{(*)}D^{(*)}$  pairs can begin to be produced, i.e. at  $(m_B + m_D) \approx 7.15$  GeV,  $(m_B + m_{D^*}) \approx 7.29$  GeV,  $(m_{B^*} + m_D) \approx 7.19$  GeV, or  $(m_{B^*} + m_{D^*}) \approx 7.33$  GeV. Subthreshold singularities arise due to the coupling to states with masses below these thresholds. On the one hand, there are cuts produced by multi-particle states. (Anomalous thresholds are seen not to appear by inspecting the relevant triangle diagrams at both quark and hadron level.) For instance, the form factor  $S_3$ , which appears in the description of  $\bar{B}^* \rightarrow D^*$  transitions, has a branch point due to its coupling to  $BD$  pairs as well as to two-particle states consisting of a  $B_c$  meson and light hadrons [17]. However, these cuts are rather short. Their effects are suppressed by phase space and, in the case of  $B_c$  states, by the Zweig rule. Once a model for the discontinuities across the cuts is adopted, these subthreshold singularities can be included in the dispersive bounds [19, 26], and their effect is found to be very small. We thus neglect these contributions in the sequel.

On the other hand, the form factors also have singularities due to single-particle states. Since both ground-state and orbitally excited  $B_c$  states are expected to be very narrow [21], we shall assume that they give poles located on the real axis. Our choice of form factors is such that the scalar functions  $S_j$  receive only contributions from scalar



particles, the vector functions  $V_j$  only from vector particles, etc., situated below the corresponding physical thresholds. The masses of these bound states have already been given in Table 1. The residues of the corresponding poles, which are proportional to the couplings of  $B_c$  states to  $B^{(*)}D^{(*)}$  pairs, are poorly known. Fortunately, dispersive bounds can still be derived even in the presence of poles with unknown residues [14, 15]. The optimal technique is to multiply each form factor  $F_j$  by a specific function  $B_j(z)$  (a so-called Blaschke or “inner” function) with zeros at the positions of the poles, and with unit modulus along the physical cut. The explicit form of the inner functions is

$$B_j(z) = \prod_n \frac{z - z_n^{(j)}}{1 - z z_n^{(j)}}, \quad (16)$$

where the index  $n$  runs over all  $B_c$  bound-states that couple to a given form factor, and

$$z_n^{(j)} = \frac{\sqrt{(m_{B^{(*)}} + m_{D^{(*)}})^2 - M_n^2} - 2a\sqrt{m_{B^{(*)}}m_{D^{(*)}}}}{\sqrt{(m_{B^{(*)}} + m_{D^{(*)}})^2 - M_n^2} + 2a\sqrt{m_{B^{(*)}}m_{D^{(*)}}}} \quad (17)$$

is the image of the pole of mass  $M_n$  in the  $z$  plane. In terms of these functions, the unitarity inequality for a given spin-parity  $J^P$  is written as

$$\frac{1}{2\pi} \int_0^{2\pi} d\theta \sum_j |f_j(e^{i\theta})|^2 \leq 1, \quad (18)$$

where

$$f_j(z) = B_j(z) \phi_j(z) F_j(w(z)) \quad (19)$$

defines analytic functions inside the unit disc. We can thus Taylor expand the functions  $f_j(z)$  in (18) and find that

$$\sum_j \sum_{n=0}^{\infty} \left| \frac{1}{n!} f_j^{(n)}(0) \right|^2 \leq 1, \quad (20)$$

where  $f_j^{(n)}(0)$  denotes the  $n$ -th derivative of  $f_j(z)$  with respect to  $z$ , evaluated at  $z = 0$ . There is one such inequality for each spin-parity channel. The derivatives with respect to  $z$  in (20) can be calculated using (19), where  $B_j(z)$  and  $\phi_j(z)$  are known functions. The derivatives of the form factors at  $z = 0$  are related to the derivatives with respect to  $w$  at the kinematical point  $w = w_0$ , defined such that  $z(w_0, a) = 0$ . For the form factor  $V_1(w)$ , for instance, we have

$$\begin{aligned} \partial_z V_1(w(z)) \Big|_{z=0} &= -8a^2 \rho_1^2 V_1(w_0), \\ \partial_z^2 V_1(w(z)) \Big|_{z=0} &= (128a^4 c_1 - 32a^2 \rho_1^2) V_1(w_0), \\ \partial_z^3 V_1(w(z)) \Big|_{z=0} &= (3072a^6 d_1 + 1536a^4 c_1 - 144a^2 \rho_1^2) V_1(w_0), \end{aligned} \quad (21)$$

where

$$w(z) = 2a^2 \left( \frac{1+z}{1-z} \right)^2 - 1, \quad (22)$$

and the parameters  $\rho_1^2$ ,  $c_1$  and  $d_1$  are defined by the expansion

$$V_1(w) = V_1(w_0) \left[ 1 - \rho_1^2(w - w_0) + c_1(w - w_0)^2 + d_1(w - w_0)^3 + \dots \right]. \quad (23)$$

Of course, the values of these parameters will depend on the choice of  $w_0$ , i.e. on the choice of the parameter  $a$  in (12).

In the heavy-quark limit, all functions  $F_j(w)$  become identical in the semileptonic region and equal to the Isgur–Wise form factor. In order to incorporate corrections to that limit, we choose the vector function  $V_1(w)$  as a reference form factor and express the expansion parameters of all other form factors in terms of the reference parameters  $\rho_1^2$ ,  $c_1$  and  $d_1$  defined above. Our choice of the reference form factor is motivated by the fact that it is the physical form factor describing the semileptonic decay  $\bar{B} \rightarrow D \ell \bar{\nu}$ . The leading symmetry-breaking corrections to the ratios of heavy-meson form factors have been analysed in great detail (for a review, see e.g. Ref. [3]). We write

$$R_j(w) \equiv \frac{F_j(w)}{V_1(w)} \equiv A_j \left[ 1 + B_j(w - w_0) + C_j(w - w_0)^2 + D_j(w - w_0)^3 + \dots \right]. \quad (24)$$

The results for the parameters  $A_j, \dots, D_j$  obtained by including the leading short-distance and  $1/m_Q$  corrections, for two different choices of  $a$  relevant to our discussion, are given in the Appendix. Using these results, the derivatives of the form factors  $F_j(w)$  can be expressed in terms of those of the reference form factor  $V_1(w)$ .

## 4 Zero-recoil expansion

A convenient choice of the parameter  $a$  in (12) is to set  $a = 1$ , in which case the conformal transformation  $w \rightarrow z$  maps the zero-recoil point  $w = 1$  onto the origin  $z = 0$  of the unit disc (i.e.  $w_0 = 1$ ). With this choice, it is straightforward to obtain bounds on the form factors and their derivatives at zero recoil. We first give the allowed values for the slope  $\rho_1^2$  and the curvature  $c_1$ , and then consider the coefficient  $d_1$  of the third-order term in (23). In order to see the effect of the corrections to the heavy-quark limit, we present the results both in the case of exact spin symmetry<sup>2</sup> and with the leading corrections taken into account. The effect of uncertainties in the corrections to the heavy-quark limit will be considered below.

When only terms with up to two derivatives are kept in inequality (20), the resulting constraint on the parameters  $\rho_1^2$  and  $c_1$  of the reference form factor is given by an ellipse [19]:

$$(\rho_1^2 - \bar{\rho}_1^2)^2 + S \left[ (c_1 - \bar{c}_1) - T(\rho_1^2 - \bar{\rho}_1^2) \right]^2 < K^2. \quad (25)$$

---

<sup>2</sup>In fact, we only equate the first three derivatives of the various form factors, but give all masses, poles and thresholds their physical values.

Table 2: *Parameters of the ellipses for the different spin–parity channels, including corrections to the heavy-quark limit*

$J^P$	$\bar{\rho}_1^2$	$\bar{c}_1$	$T$	$S$	$K$	$\varphi$
$0^+$	0.58	0.42	1.08	44.3	1.05	$47.5^\circ$
$0^-$	0.87	0.81	1.12	61.9	1.13	$48.4^\circ$
$1^-$	0.86	0.80	1.14	62.9	3.84	$48.9^\circ$
$1^+$	0.95	0.85	1.42	39.0	3.92	$55.0^\circ$

The single parameter sensitive to the values of the QCD correlators given in (11) is the “radius”  $K$ . All other parameters of the ellipse depend on known meson masses and, to a lesser extent, on the symmetry-breaking corrections of (24). In Figure 1, we show the resulting ellipses for the different spin–parity channels, both with and without corrections to the heavy-quark limit. Only values of the parameters inside the ellipses are permitted. The effects of the corrections to the heavy-quark limit are small and tend to align the major axes of the four ellipses. In Table 2, we give the corresponding ellipse parameters, including the angle  $\varphi$  of the major axis. In all four cases, we find that  $S \approx 40\text{--}60$ , implying that the ellipses are highly degenerate. As a consequence, the curvature parameter  $c_1$  is strongly correlated with the slope parameter  $\rho_1^2$ , a model-independent property observed in Ref. [19]. It is apparent from Figure 1 that the bounds derived from the  $0^\pm$  channels are much stronger than (and fully contained in) those derived from the  $1^\pm$  channels. Therefore, we will not consider the latter hereafter. For completeness, we note that the (axial) vector and the (pseudo) scalar form factors are not fully independent functions, since some of them have to obey kinematical constraints at the point of maximum recoil, corresponding to  $q^2 = 0$ . When deriving the dispersive bounds in the different spin–parity channels, the kinematical constraints can be incorporated using Lagrange multipliers. The dispersive bounds derived in the (pseudo) scalar channel are then interconnected with those derived in the (axial) vector channel, yielding a domain for the parameters of the reference form factor that is smaller than the one obtained from the intersection of the allowed domains obtained separately from the different spin–parity channels. In practice, however, the (pseudo) scalar channel yields so much more restrictive bounds than the (axial) vector channel that the resulting improvement is negligible.

To see what happens when the term with three derivatives is included, consider the simpler case of only a single form factor contributing to the unitarity sum. Then the corresponding inequality can be written in a form similar to (25):

$$(\rho_1^2 - b_1)^2 + (8c_1 - b_2 - b_3\rho_1^2)^2 + (64d_1 - b_4 - b_5\rho_1^2 - b_6c_1)^2 < K^2, \quad (26)$$

where the  $b_i$  are numerical coefficients. This relation describes a highly degenerate

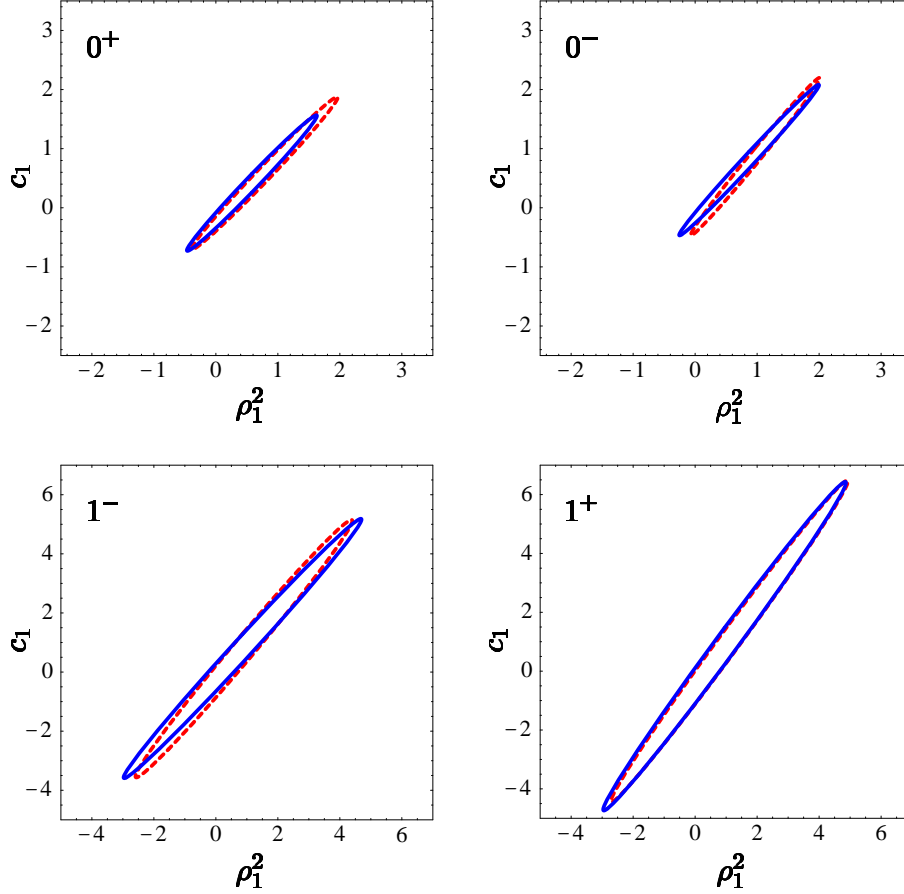


Figure 1: *Bounds on the slope and curvature of the reference form factor  $V_1(w)$  obtained from the unitarity inequalities in the different spin–parity channels. Dashed curves correspond to the heavy-quark limit, while solid ones include the leading corrections to that limit. Note that the axes in the lower plots are extended by a factor of 2.*

ellipsoid in  $(\rho_1^2, c_1, d_1)$  space, whose axes are roughly in the ratios  $1 : 1/8 : 1/64$ . The coefficient  $d_1$  is thus determined within a rather small range:

$$d_1 = \frac{b_4 + b_5 \rho_1^2 + b_6 c_1}{64} \pm \Delta, \quad (27)$$

where  $\Delta < K/64 \approx 0.02$ . We will see below that this is much smaller than the range due to the theoretical uncertainty in the relations between the various form factors. What changes in the general case of many form factors are the precise values of the coefficients 8 and 64 in front of  $c_1$  and  $d_1$ , as well as the values of the other ellipsoid parameters. In addition, the inclusion of the third derivative in (20) reduces the allowed domain for the first two derivatives. This feature is specific to the simultaneous treatment of several form factors whose derivatives are related, as they are here through heavy-quark symmetry. However, the inclusion of many form factors does not change the strong degeneracy of the ellipsoid in  $(\rho_1^2, c_1, d_1)$  space.

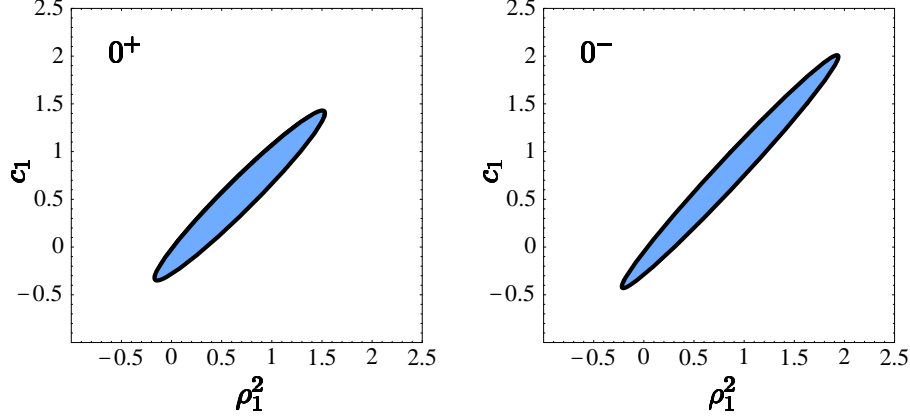


Figure 2: *Bounds on the slope and curvature of the reference form factor  $V_1(w)$  obtained by including the third-derivative terms in the unitarity inequalities for the  $0^\pm$  channels, taking theoretical uncertainties in the calculation of corrections that break heavy-quark symmetry into account.*

Table 3: *Parameters of the ellipses obtained from the third-order inequalities, including theoretical uncertainties. We also quote results for the third-order coefficient  $d_1 = \alpha\rho_1^2 + \beta c_1 + \gamma$ .*

$J^P$	$\bar{\rho}_1^2$	$\bar{c}_1$	$T$	$S$	$K$	$\varphi$	$\alpha$	$\beta$	$\gamma$
$0^+$	0.68	0.54	1.01	14.9	0.85	46.2°	0.47(11)	-1.33(6)	0.01(11)
$0^-$	0.86	0.79	1.11	29.2	1.08	48.4°	0.44(10)	-1.37(6)	0.05(11)
Combined	0.67	0.55	1.03	25.9	0.84	46.4°	0.45(7)	-1.35(4)	0.03(8)

At first sight, the inclusion of the third derivative terms bring an improvement which appears to be very significant. For the case of the  $0^+$  channel, for instance, the resulting allowed region for the parameters  $\rho_1^2$  and  $c_1$  is reduced, with respect to the one shown in Figure 1, by more than a factor of 3. However, the situation changes if we allow for theoretical errors  $\delta B_j$ ,  $\delta C_j$  and  $\delta D_j$  in the coefficients entering the relations (24) between the various form factors.<sup>3</sup> To this end, we generate a large number of ellipses by taking random values of the theoretical errors within intervals  $[-\delta B, \delta B]$ ,  $[-\delta C, \delta C]$ , and  $[-\delta D, \delta D]$ , setting  $\delta B = \delta C = \delta D = 0.1$ , which we believe is a conservative estimate of the uncertainties. The results are shown in Figure 2. Whereas the effect of theoretical uncertainties is moderate in the case of the second-order inequality, it has a large impact at third order. The envelope of the ellipses obtained in that case is much larger than each single ellipse, and almost fills up the ellipse obtained at second order. This shows that

<sup>3</sup>There is no need to include errors in the normalization of the form factors at zero recoil, since we have already used a conservative low value for the normalization of the reference form factor.

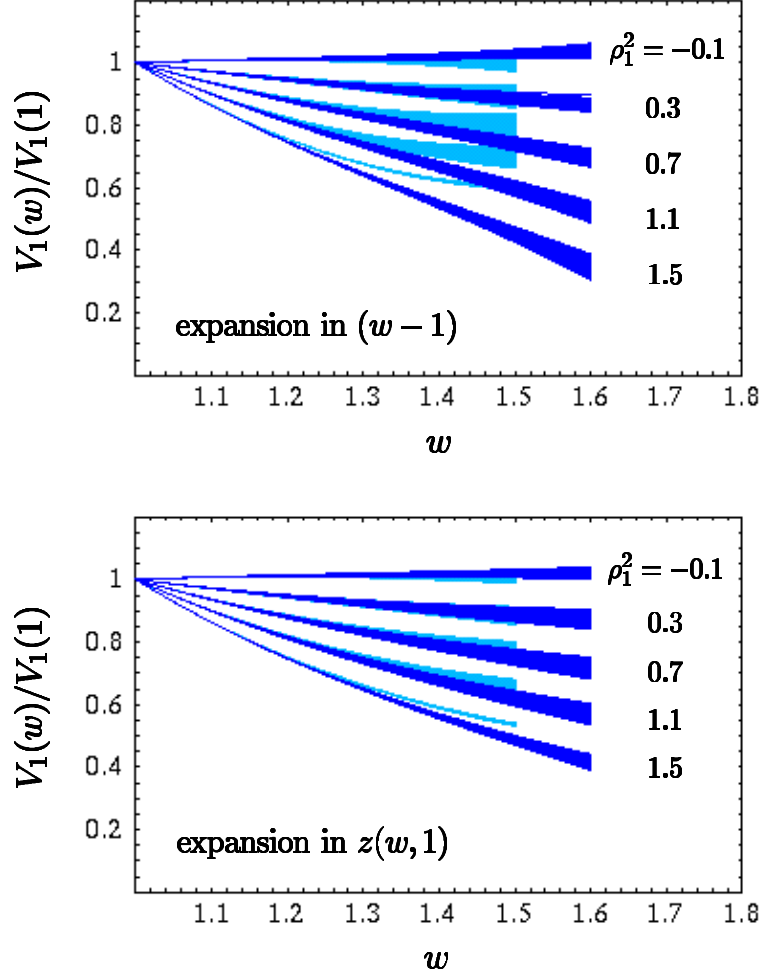


Figure 3: Allowed shapes of the function  $V_1(w)$  for various values of  $\rho_1^2$ . The dark (light) bands correspond to the third-order (second-order) expansion of the form factor. In the upper plot, the expansion is performed in powers of  $(w - 1)$ , in the lower plot in powers of the variable  $z(w, 1)$ .

not much can be gained by going to yet higher orders in the expansion. The thick ellipses in Figure 2 are a good approximation to the allowed regions. The parameters of these ellipses are given in Table 3. Their intersection is again to excellent approximation given by an ellipse, whose parameters are given in the last row. We also present the results for the third-order expansion coefficient  $d_1$ , which we write as  $d_1 = \alpha\rho_1^2 + \beta c_1 + \gamma$ . We find that the allowed range for this parameter obtained from (27) is only little affected by theoretical errors. The consistency between the results obtained from the two channels allows us to take the average of the two results, shown in the last row.

To exhibit the possible behaviour of the form factor  $V_1(w)$  predicted by our results, we show in the upper plot in Figure 3 the allowed shapes for this function for a selection of equally spaced values of the slope parameter  $\rho_1^2$  inside the allowed region, given by

$-0.17 < \rho_1^2 < 1.51$ . For each choice of  $\rho_1^2$ , the parameters  $c_1$  and  $d_1$  are scanned over the regions allowed by the dispersive bounds. The results are shown with and without including the third-order term in the zero-recoil expansion, i.e. the expansion in (23) with  $w_0 = 1$ . Close to zero recoil (i.e. for  $1 \leq w < 1.2$ ), both approximations provide an equally accurate description of the form factor. For larger recoil, the effect of the third-order term becomes clearly visible. The convergence rate of the series can be improved by expressing the form factor  $V_1(w(z))$ , with  $w(z)$  given in (22), as a power series in  $z$  rather than in  $(w - 1)$ . The corresponding results are shown in the lower plot in Figure 3. Now the differences between the second- and third-order expansions become important only at larger values of  $w$ , and we are confident that the third-order results provide an adequate representation of the form factor over the entire kinematical region accessible in semileptonic decays. Because the spread in the curves caused by variations of the parameter  $c_1$  and  $d_1$  inside the allowed regions is very small, our results can be represented, to a very good approximation, by taking the values of these parameters along the major axes. This gives the one-parameter function

$$\frac{V_1(w)}{V_1(1)} \approx 1 - 8\rho_1^2 z + (51.\rho_1^2 - 10.)z^2 - (252.\rho_1^2 - 84.)z^3,$$

$$\text{with } z = \frac{\sqrt{w+1} - \sqrt{2}}{\sqrt{w+1} + \sqrt{2}}. \quad (28)$$

As an aside, we note that expanding this result in powers of  $(w - 1)$  would yield the slope-curvature relation  $c_1 \approx 1.05\rho_1^2 - 0.15$ , which is not very different from the relation  $c_1 \approx 0.74\rho_1^2 - 0.09$  obtained in Ref. [19] with some assumptions about subthreshold singularities. We stress, however, that in the present work such assumptions are avoided.

## 5 Optimized expansion

We have seen above that higher-order terms in the expansion of the form factor  $V_1(w)$  around the zero-recoil point have a significant effect already for rather small values of  $w$ . The convergence of the expansion was improved considerably by introducing the variable  $z$  instead of  $(w - 1)$ ; however, the question arises whether an even better convergence can be achieved by optimizing the choice of the expansion variable.

When one wishes to approximate a function along an interval, the most natural expansion is given in terms of orthonormal polynomials on this interval. The domain of convergence of the expansion is then an ellipse passing through the first singularity of the function [27]. In order to accelerate the rate of convergence in the interval of interest, one must conformally map the interior of the function's analyticity domain onto the inside of an ellipse, such that the interval of interest is applied to the segment between the focal points [28]. This conformal mapping is given by elliptic functions [29]. However, when the physical interval is far from the first singularity (as it is for semileptonic  $\bar{B}^{(*)} \rightarrow D^{(*)}$  decays), the ellipse is almost degenerate to a circle, so that a simple Taylor expansion about the center of the ellipse will have almost the same

radius of convergence as the expansion in orthonormal polynomials discussed above. In the absence of subthreshold singularities, this approximate circle is simply a rescaling of the circle obtained using the conformal mapping of (12), with  $a$  determined such that the physical region is applied onto an interval symmetric about the origin  $z = 0$ . This gives  $a = a_{\text{opt}}$  such that  $z(w_{\text{max}}, a_{\text{opt}}) = -z(1, a_{\text{opt}})$ , which is very close to the variable first suggested by Boyd and Lebed [30]. For the case of  $\bar{B} \rightarrow D$  transitions, we find  $a_{\text{opt}} \approx 1.067$  and  $z_{\text{max}} \equiv z(w_{\text{max}}, a_{\text{opt}}) \approx 0.032$ .

The argument just presented is only valid when there are no subthreshold singularities, while the form factors of interest have poles and branch points below the physical cut. Nevertheless, because the singularities are far from the semileptonic domain, the variable  $z(w, a_{\text{opt}})$  remains an excellent choice. Indeed, a measure of the rate of convergence of an expansion of a form factor in a variable  $x$  is provided by the ratio  $r_{\text{conv}} = |x|_{\text{max}}/|x|_{\text{pole}}$  where  $x_{\text{pole}}$  is the position of the first pole and  $|x|_{\text{max}}$  the largest value  $|x|$  can take in the semileptonic domain. The form factor  $S_1(w)$ , for instance, has a pole due to a scalar state at 6.70 GeV, so that  $r_{\text{conv}} \approx 0.07$ . For comparison, we note that  $r_{\text{conv}} \approx 0.35$  for the expansion variable  $x = (w - 1)$ , and  $r_{\text{conv}} \approx 0.15$  for the variable  $x = z(w, 1)$  used in the previous section. It is clear that  $z(w, a_{\text{opt}})$  gives the best rate of convergence. In order to simplify notation in what follows, we will write  $z_*$  for  $z(w, a_{\text{opt}})$  and  $a_*$  for  $a_{\text{opt}}$ . We shall use the same value of  $a_*$  for all form factors.

Our claim is that all  $\bar{B}^{(*)} \rightarrow D^{(*)}$  form factors can be accurately described by a second-order polynomial in  $z_*$ . In particular, we shall derive dispersive constraints on the slope  $\rho_{1*}^2$  and the curvature  $c_{1*}$  (now taken at the recoil point  $w = w_0 \approx 1.276$ ) in the expansion of the reference form factor  $V_1(w(z_*))$ , i.e.

$$\frac{V_1(w)}{V_1(w_0)} \approx 1 - 8a_*^2\rho_{1*}^2z_* + 16a_*^2(4a_*^2c_{1*} - \rho_{1*}^2)z_*^2. \quad (29)$$

To estimate the truncation error due to the neglect of higher-order terms, consider the expansion of the analytic functions  $f_j(z)$  of (19) around  $z = 0$ . If we write

$$f_j(z) = f_j(0) \left( 1 + \frac{f_j^{(1)}(0)}{f_j(0)} z + \frac{f_j^{(2)}(0)}{f_j(0)} \frac{z^2}{2} + \Delta_j(z) \right), \quad (30)$$

the remainder  $\Delta_j(z)$  can be bounded using the dispersive constraint (20). We find that

$$|\Delta_j(z)| < |z|^3 \sqrt{\frac{1}{|f_j(0)|^2} - 1}. \quad (31)$$

Let us concentrate, for concreteness, on the scalar form factor  $S_1(w)$ . Making the conservative assumption that  $S_1(w_0)$  is as low as  $\frac{2}{3} S_1(1)$ , we find  $|\Delta_{S_1}(z)| < 7 \times 10^{-4}$  for all values of  $z$  corresponding to the semileptonic region. This truncation error is tiny and will be neglected in what follows. The second step consists in noticing that the known function  $[\phi_{S_1}(z_*)B_{S_1}(z_*)]^{-1}$  is well approximated by a second-order polynomial in  $z_*$ . This is where the convergence criterion discussed earlier comes into play, since



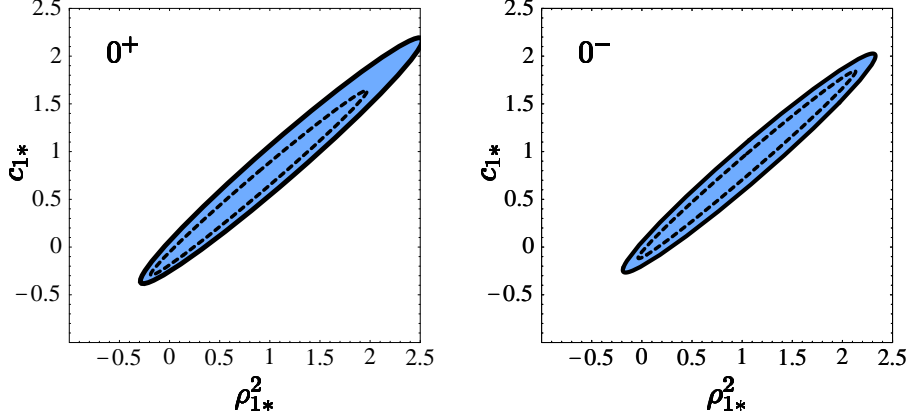


Figure 4: *Bounds on the slope and curvature of the reference form factor  $V_1(w)$  obtained using an expansion in the optimized variable  $z_*$ . The solid (dashed) ellipses show the results obtained with (without) including theoretical uncertainties in the heavy-quark relations.*

$1/B_{S_1}(z_*)$  contains the scalar poles. The fact that  $r_{\text{conv}} = |z_*|_{\text{max}}/|z_{*\text{pole}}|$  is so small guarantees that the expansion of  $[\phi_{S_1}(z_*)B_{S_1}(z_*)]^{-1}$  converges rapidly. We find that the first three terms in this expansion deviate by at most 0.2% from the full function over the whole semileptonic region. As a result, the form factor  $S_1(w)$ , which is proportional to the product of the two quantities  $f_{S_1}(z_*)$  and  $[\phi_{S_1}(z_*)B_{S_1}(z_*)]^{-1}$ , is approximated to an accuracy of better than about 0.2% by the product of the truncated expansions of these two factors. Of course, this product includes terms of order  $z_*^3$  and  $z_*^4$ . However, their contribution never exceeds 1.5% over the full semileptonic region (it is lower than 1% in the region  $w < 1.5$ ). Thus, we conclude that the scalar form factor  $S_1(w)$  can be described by a second-order polynomial in  $z_*$  with an accuracy of better than 2%. A similar conclusion holds for all other  $\bar{B} \rightarrow D^{(*)}$  form factors, since they are related to the  $S_1(w)$  by heavy-quark symmetry, up to small corrections.

As in Section 4, we use the dispersive bounds to constrain the first two derivatives of  $V_1(w)$  at  $w_0$ . However,  $w_0$  is not the zero-recoil point here, and the left-hand side of (20) contains as an overall factor the unknown normalization  $|V_1(w_0)|^2$ . To proceed, we multiply both sides of the inequality by a common factor,

$$\left| \frac{V_1(1)}{V_1(w_0)} \right|^2 \sum_j \sum_{n=0}^{\infty} \left| \frac{1}{n!} f_j^{(n)}(0) \right|^2 \leq \left| \frac{V_1(1)}{V_1(w_0)} \right|^2, \quad (32)$$

such that now the left-hand side contains the known normalization  $V_1(1)$ . To evaluate the right-hand side of (32) we rely on our observation that in the semileptonic region all  $\bar{B}^{(*)} \rightarrow D^{(*)}$  form factors are very well described by a second-order polynomial in  $z_*$ , and thus use (29) with  $w = 1$ . This approximation enables us to write the resulting constraints on  $\rho_{1*}^2$  and  $c_{1*}$  as ellipses, like in the zero-recoil case.

For the scalar and pseudoscalar channels, the ellipses obtained in the  $(\rho_{1*}^2, c_{1*})$  plane are shown in Figure 4. The dashed ones correspond to using the central values of the

Table 4: *Parameters of the ellipses obtained from the second-order inequalities, using the optimized variable  $z_*$*

$J^P$	$\bar{\rho}_1^2$	$\bar{c}_1$	$T$	$S$	$K$	$\varphi$
$0^+$	1.11	0.89	0.90	29.0	1.40	$42.5^\circ$
$0^-$	1.07	0.88	0.89	27.6	1.26	$42.2^\circ$

parameters  $A_j$ ,  $B_j$  and  $C_j$  defined in (24) and given in the Appendix. As in Section 4, we account for theoretical uncertainties in the values of these parameters by generating a large number of ellipses, allowing  $B_j$  and  $C_j$  to vary by  $\pm 0.1$ . This procedure generates the shaded areas, which to a good approximation are contained in the larger ellipses. We find again a similarity between the final ellipses in the two channels and, in particular, a near alignment of their major axes. The intersection of these two ellipses is, to a very good approximation, given by the pseudoscalar ellipse alone. This is in contrast to the zero-recoil expansion considered in the previous section, where it was the scalar channel that gave the tighter constraints. For completeness, the ellipse parameters are given in Table 4.

Let us now investigate the properties of the optimized parametrization and compare them with the results obtained in the previous section. In the upper plot in Figure 5, we show the allowed shapes of the form factor  $V_1(w)$  for values of the slope parameter  $\rho_{1*}^2$  chosen such that they correspond to the values of the zero-recoil slope  $\rho_1^2$  used in Figure 3. For each choice of  $\rho_{1*}^2$ , the parameter  $c_{1*}$  is scanned over the region allowed by the dispersive bounds. Because  $S$  is large compared with  $K^2$ , and because the term multiplying  $c_{1*}$  in expression (29) for the form factor is suppressed by the small factor  $z_*^2$ , the spread in the curves caused by the variation of  $c_{1*}$  is very small. Therefore, to a very good accuracy,  $c_{1*}$  can be replaced by  $\bar{c}_1 + \tan \varphi (\rho_{1*}^2 - \bar{\rho}_1^2)$ . This gives the one-parameter function

$$\frac{V_1(w)}{V_1(1)} \approx \frac{1 - 9.105\rho_{1*}^2 z_* + (57.0\rho_{1*}^2 - 7.5)z_*^2}{0.354\rho_{1*}^2 + 0.992},$$

$$\text{with } z_* = \frac{\sqrt{w+1} - 1.509}{\sqrt{w+1} + 1.509}. \quad (33)$$

The light-shaded bands in the figure include, in addition to the spread discussed above, an estimate of the truncation error due to the neglect of higher-order terms in  $z_*$ . It is obtained by not expanding the known functions  $[\phi_j(z_*)B_j(z_*)]^{-1}$  in powers of  $z_*$ , but keeping their full expressions to calculate the form factors from the second-order expansions of the functions  $f_j(z_*)$ . (We have argued above that the error from the truncation of the functions  $f_j(z_*)$  themselves is a negligible effect.) These bands reflect the total theoretical uncertainty in our results, which is seen never to exceed the level

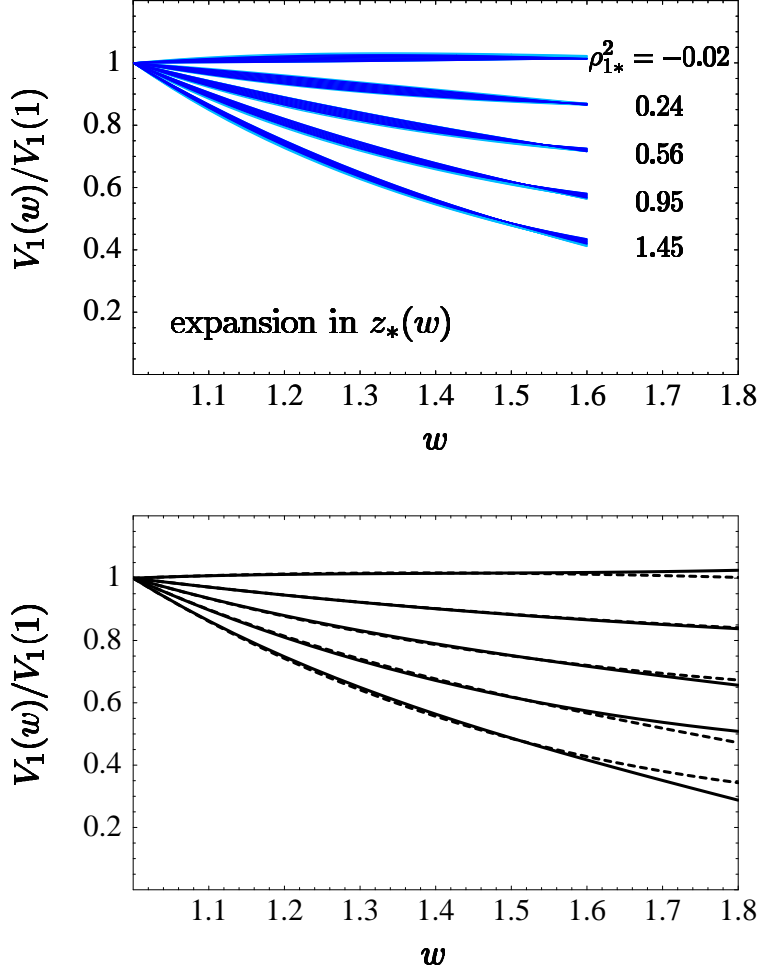


Figure 5: *Upper plot: Allowed shapes for the function  $V_1(w)$  for various values of  $\rho_{1*}^2$  (the slope at  $w_0 \approx 1.276$ ) chosen such that they correspond to the values of  $\rho_1^2$  (the slope at  $w = 1$ ) of Figure 3. The light bands include an estimate of the truncation error. Lower plot: Comparison of the two one-parameter approximations (28) (solid) and (33) (dashed).*

of 2%. As a consequence, the one-parameter description of the form factor given above can be trusted to that level of precision.

In the lower plot in Figure 5, we compare the parametrization (33) to the one given in (28). The parameters  $\rho_1^2$  and  $\rho_{1*}^2$  are chosen as before. We find that the two sets of curves are nearly indistinguishable in the semileptonic region  $1 \leq w < 1.6$ , whereas they start to diverge for larger  $w$  values. This agreement provides a strong consistency check of our method, given that the expansions in the two variables  $z$  and  $z_*$  are carried out to different order, and that the dispersive bounds in the two cases are dominated by different spin-parity channels. We thus conclude that, for all practical purposes, both parametrizations are equally reliable. Similar parametrizations for all other  $\bar{B}^{(*)} \rightarrow D^{(*)}$  form factors can be obtained using (24) and the results given in the Appendix.

## 6 Phenomenological applications

We now summarize our results and provide simple, constrained parametrizations for the form factors which determine the differential rates for  $\bar{B} \rightarrow D \ell \bar{\nu}$  and  $\bar{B} \rightarrow D^* \ell \bar{\nu}$  decays. The form factor  $V_1(w)$  governing the first process is described to an accuracy of better than 2% by the two parametrizations given in (28) and (33). The two slope parameters entering these expressions are related by

$$\rho_{1*}^2 \approx \frac{0.62\rho_1^2 + 0.04}{1 - 0.22\rho_1^2}, \quad \rho_1^2 \approx \frac{1.61\rho_{1*}^2 - 0.06}{1 + 0.36\rho_{1*}^2}. \quad (34)$$

The dispersive bounds discussed in Section 4 require that  $-0.17 < \rho_1^2 < 1.51$ , and therefore  $-0.07 < \rho_{1*}^2 < 1.47$ . These intervals, by themselves, represent nontrivial bounds on the slope of the form factor, which are competitive with the most recent bounds derived from inclusive heavy-quark sum rules [31].

To obtain similar parametrizations of the function  $\mathcal{F}(w)$ , which governs the  $\bar{B} \rightarrow D^* \ell \bar{\nu}$  decay rate in (1), we find it convenient to first relate this function to the axial-vector form factor  $A_1(w)$  through [3]

$$\left[1 + \frac{4w}{w+1} \frac{1 - 2wr + r^2}{(1-r)^2}\right] \mathcal{F}(w)^2 = \left\{2 \frac{1 - 2wr + r^2}{(1-r)^2} \left[1 + \frac{w-1}{w+1} R_1(w)^2\right] + \left[1 + \frac{w-1}{1-r} (1 - R_2(w))\right]^2\right\} A_1(w)^2, \quad (35)$$

where  $r = m_{D^*}/m_B$ , and  $R_1(w)$  and  $R_2(w)$  are ratios of form factors defined in the Appendix, and are given by

$$R_1(w) = \frac{h_V(w)}{h_{A_1}(w)} \approx 1.27 - 0.12(w-1) + 0.05(w-1)^2, \\ R_2(w) = \frac{h_{A_3}(w) + r h_{A_2}(w)}{h_{A_1}(w)} \approx 0.80 + 0.11(w-1) - 0.06(w-1)^2. \quad (36)$$

The theoretical predictions for these ratios are supported by measurements reported by the CLEO Collaboration [32]. We have chosen to work with  $A_1(w)$  instead of  $\mathcal{F}(w)$ , because the latter suffers from large kinematical enhancements of the corrections to the heavy-quark limit. In other words, the coefficients in the expansion of the ratio  $\mathcal{F}(w)/V_1(w)$  corresponding to (37) below would be large. These large corrections were not accounted for in Ref. [20], where the symmetry-breaking corrections in the relation between  $\mathcal{F}(w)$  and  $A_1(w)$  are neglected.

Using the results of the Appendix, the form factor  $A_1(w)$  can be related to the reference form factor  $V_1(w)$  through

$$\frac{A_1(w)}{V_1(w)} \approx 0.948(1 - 0.212z - 4.007z^2 - 1.342z^3 + \dots) \\ \approx 0.937(1 - 0.476z_* - 4.163z_*^2 + \dots), \quad (37)$$

Table 5: *Results of the various fits to experimental data on the recoil spectra in  $\bar{B} \rightarrow D^* \ell \bar{\nu}$  decays [34]. The slope parameters are measured at  $w = 1$ .*

Parametrization	$ V_{cb}  \mathcal{F}(1)$	$\rho_{A_1}^2$	$\rho_{\mathcal{F}}^2$
Eq. (38)	0.037(2)	1.36(18)	1.15(18)
Eq. (39)	0.037(2)	1.34(17)	1.13(17)
Linear Fit	0.035(2)	—	0.81(13)

where  $z = z(w, 1)$  and  $z_* = z(w, a_*)$ . From this, it is straightforward to derive the parametrizations of  $A_1(w)$  from the results for  $V_1(w)$  given in (28) and (33). They are

$$\frac{A_1(w)}{A_1(1)} \approx 1 - 8\rho_{A_1}^2 z + (53.\rho_{A_1}^2 - 15.)z^2 - (231.\rho_{A_1}^2 - 91.)z^3,$$

$$\text{with } z = \frac{\sqrt{w+1} - \sqrt{2}}{\sqrt{w+1} + \sqrt{2}}, \quad (38)$$

and

$$\frac{A_1(w)}{A_1(1)} \approx \frac{1 - 9.105\rho_{A_1*}^2 z_* + (61.3\rho_{A_1*}^2 - 14.8)z_*^2}{0.358\rho_{A_1*}^2 + 0.984},$$

$$\text{with } z_* = \frac{\sqrt{w+1} - 1.509}{\sqrt{w+1} + 1.509}. \quad (39)$$

The relation between the two slope parameters entering these expressions is

$$\rho_{A_1*}^2 \approx \frac{0.60\rho_{A_1}^2 + 0.07}{1 - 0.22\rho_{A_1}^2}, \quad \rho_{A_1}^2 \approx \frac{1.66\rho_{A_1*}^2 - 0.12}{1 + 0.36\rho_{A_1*}^2}. \quad (40)$$

The dispersive bounds discussed in Section 4 require that  $-0.14 < \rho_{A_1}^2 < 1.54$  and  $-0.01 < \rho_{A_1*}^2 < 1.51$ . Alternatively, we could repeat the derivation of the dispersive bounds using  $A_1(w)$  instead of  $V_1(w)$  as the reference form factor. Since the symmetry-breaking corrections in the relation between the two form factors are very small, the two procedures give essentially the same results.

Our results will eliminate the large uncertainty associated with the extrapolation of the experimental recoil spectra in  $\bar{B} \rightarrow D^{(*)} \ell \bar{\nu}$  decays to zero recoil. At present, this uncertainty is the main experimental error in the determination of  $|V_{cb}|$  [33]. In fact, in many experimental analyses a linear shape of the form factor has been used to extrapolate the data, without attributing an error to this assumption. A reanalysis using our constrained parametrizations is therefore highly desirable in order to get a reliable determination of  $|V_{cb}|$ . To illustrate the potential impact of our results, we show in

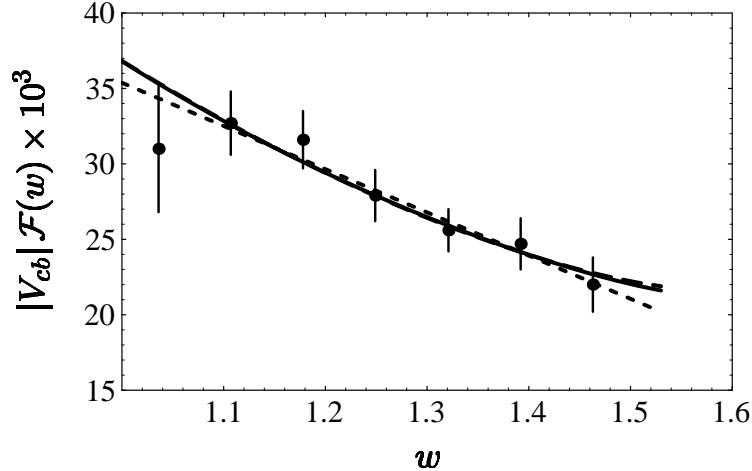


Figure 6: Experimental data for the product  $|V_{cb}| \mathcal{F}(w)$  as a function of  $w$ , extracted from semileptonic  $\bar{B} \rightarrow D^* \ell \bar{\nu}$  decays [34]. The solid curve is a fit using our parametrization in (38), while the (barely visible) long-dashed one refers to the parametrization of (39). The two curves are nearly indistinguishable in the semileptonic domain. The short-dashed line shows a straight-line fit, similar to the one used in the experimental analysis.

Figure 6 different fits to the data for the product  $\mathcal{F}(w) |V_{cb}|$  measured in  $\bar{B} \rightarrow D^* \ell \bar{\nu}$  decays by the CLEO Collaboration [34]. Similar measurements have also been reported in Refs. [35]–[38]. Our goal here is not to establish a new value of  $|V_{cb}|$  (which is best done by the experimental collaborations themselves), but rather to illustrate how our parametrizations work. The short-dashed line shows a linear fit to the data, whereas the solid and long-dashed curves show the fits obtained using our parametrizations. All fits have an excellent  $\chi^2/\text{dof}$  between 0.3 and 0.4, reflecting that we are neglecting correlations between the errors of the various data points. Clearly, the two parametrizations we propose give nearly indistinguishable fits. More importantly, the obtained values of  $|V_{cb}|$  and the zero-recoil slope parameters are systematically larger than those derived from the linear fits.

The results of the fits are summarized in Table 5, where we also quote values for the slopes of the form factors  $A_1(w)$  and  $\mathcal{F}(w)$  at zero recoil. The theoretical prediction for the difference between the two slope parameters, which can be derived using the results of the Appendix, is  $\rho_{\mathcal{F}}^2 \approx \rho_{A_1}^2 - 0.21$  [3].

## 7 Conclusions

We have derived dispersive bounds on the shape of the form factors describing semileptonic  $\bar{B} \rightarrow D^{(*)} \ell \bar{\nu}$  decays. The method we use is based on dispersion relations and complex-analysis techniques, which combine QCD calculations of current–current correlation functions in the Euclidean domain with spectral representations of these functions

in terms of sums over intermediate hadronic states. Using the positivity of these spectral functions and crossing symmetry, it is possible to derive bounds on the form factors of particular hadron states that are contained in the spectral sum. In the case of heavy mesons, these bounds can be strengthened by including in the unitarity sum all contributions that are related, in the semileptonic region, by heavy-quark spin symmetry. Thus, we include the contributions of  $BD$ ,  $BD^*$ ,  $B^*D$  and  $B^*D^*$  states, taking into account the leading short-distance and  $1/m_Q$  corrections to the heavy-quark limit. We consider all four spin-parity channels relevant for  $\bar{B}^{(*)} \rightarrow D^{(*)}$  transitions and combine them in an optimal way.

We first apply these methods to derive bounds on the slope, curvature and third derivative of a reference form factor in an expansion around the zero-recoil point  $w = 1$ , using as input the value of this form factor at zero recoil. We find that a consistent inclusion of the third-derivative term requires a careful treatment of theoretical uncertainties in the relations that connect various form factors in the heavy-quark limit. We show explicitly how accounting for these uncertainties reduces significantly the apparent improvement brought by the third-derivative term.

In analysing the different spin-parity channels, we find that the scalar and pseudoscalar channels give significantly better bounds than the vector and axial-vector ones. We find a strong correlation between the curvature and slope of the reference form factor, and an even stronger correlation of the third derivative with the slope and curvature. This observation has led us to investigate expansions in other kinematical variables, in which the strong correlations between the parameters of the  $(w - 1)$  expansion are explained naturally. We find that the variable  $z(w, a)$  defined in (12) accomplishes this task, and furthermore leads to an improved convergence of the expansion of the form factors. We have discussed two choices of the parameter  $a$  that are particularly convenient: the choice  $a = 1$  leads to an expansion around zero recoil, however in a better variable than  $(w - 1)$ ; the choice  $a = a_*$  discussed in Section 5 corresponds to an expansion around a kinematical point close to the center of the semileptonic region, thus providing nearly optimal convergence. For the first choice, we find that the scalar channel provides the tightest constraints, and that the form factors can be well approximated by third-order polynomials. For the second choice, the pseudoscalar channel gives the best bounds, and the form factors can be approximated by second-order polynomials. In both cases, we derive simple one-parameter functions for the physical form factors  $V_1(w)$  and  $A_1(w)$ , which are accurate to better than 2% in the semileptonic region. Similar parametrizations for all other  $\bar{B}^{(*)} \rightarrow D^{(*)}$  form factors can be obtained using (24) and the results given in the Appendix. The fact that the parametrizations obtained in the two cases lead to shapes of the form factors that are nearly indistinguishable in the semileptonic region provides a strong consistency check of the method. We note that our functions are simpler than those derived by Boyd et al. [20] and include the leading short-distance and  $1/m_Q$  corrections to the heavy-quark limit, as well as the uncertainties in their calculation. Nevertheless, we have checked that in fits to available experimental data our results for the form factors agree with those obtained in Ref. [20] to better than 3% for values  $w < 1.5$ . For larger values of  $w$ , the parametrization for  $\mathcal{F}(w)$  given in this

reference becomes less reliable.

For the convenience of the reader, we restate our results obtained in the zero-recoil expansion based on the variable  $z(w, 1)$ , which gives the simplest parametrizations. They are

$$\begin{aligned}\frac{V_1(w)}{V_1(1)} &\approx 1 - 8\rho_1^2 z + (51.\rho_1^2 - 10.)z^2 - (252.\rho_1^2 - 84.)z^3, \\ \frac{A_1(w)}{A_1(1)} &\approx 1 - 8\rho_{A_1}^2 z + (53.\rho_{A_1}^2 - 15.)z^2 - (231.\rho_{A_1}^2 - 91.)z^3,\end{aligned}\tag{41}$$

where  $z = (\sqrt{w+1} - \sqrt{2})/(\sqrt{w+1} + \sqrt{2})$ , and  $\rho_1^2$  and  $\rho_{A_1}^2$  are the slope parameters at zero recoil, restricted to the intervals  $-0.17 < \rho_1^2 < 1.51$  and  $-0.14 < \rho_{A_1}^2 < 1.54$ . The values of the form factors at zero recoil are known to be  $V_1(1) = 0.98 \pm 0.07$  and  $A_1(1) = 0.91 \pm 0.03$ . In Section 6, we have shown how these results can be used to determine  $|V_{cb}|$  from an extrapolation of experimental data on semileptonic decays to zero recoil. Not only do our parametrizations eliminate the main experimental uncertainty in this extraction, but they also lead to a corrected value for  $|V_{cb}|$  that is systematically higher (by about one standard deviation) than the value obtained from a linear fit.

*Acknowledgments:* One of us (I.C.) is grateful to the CERN Theory Division, and to Centre de Physique des Particules de Marseille, for the hospitality extended to her during part of this work. We thank the authors of Ref. [20] for communicating results of their work prior to publication, and David Rousseau for useful discussions.



## Appendix: Form factors and heavy-quark relations

In the context of the heavy-quark expansion, it is common practice to parametrize the meson matrix elements of the weak currents  $V^\mu = \bar{c}\gamma^\mu b$  and  $A^\mu = \bar{c}\gamma^\mu\gamma^5 b$  by a set of form factors  $h_i(w)$  that depend on the kinematical variable  $w = v \cdot v'$ , where  $v$  and  $v'$  are the meson velocities. With a mass-independent normalization of meson states, these functions are defined as [5]

$$\begin{aligned}
\langle D(v')|V^\mu|\bar{B}(v)\rangle &= h_+(w)(v+v')^\mu + h_-(w)(v-v')^\mu, \\
\langle D^*(v',\varepsilon')|V^\mu|\bar{B}(v)\rangle &= ih_V(w)\epsilon^{\mu\nu\alpha\beta}\varepsilon'_\nu v'_\alpha v_\beta, \\
\langle D(v')|V^\mu|\bar{B}^*(v,\varepsilon)\rangle &= ih_{\bar{V}}(w)\epsilon^{\mu\nu\alpha\beta}\varepsilon_\nu v'_\alpha v_\beta, \\
\langle D^*(v',\varepsilon')|V^\mu|\bar{B}^*(v,\varepsilon)\rangle &= -\left[h_1(w)(v+v')^\mu + h_2(w)(v-v')^\mu\right]\varepsilon'^*\cdot\varepsilon \\
&\quad + h_3(w)\varepsilon'^*\cdot v\varepsilon^\mu + h_4(w)\varepsilon\cdot v'\varepsilon'^*\mu \\
&\quad - \left[h_5(w)v^\mu + h_6(w)v'^\mu\right]\varepsilon'^*\cdot v\varepsilon\cdot v', \tag{A.1}
\end{aligned}$$

for the vector current, and

$$\begin{aligned}
\langle D^*(v',\varepsilon')|A^\mu|\bar{B}(v)\rangle &= h_{A_1}(w)(w+1)\varepsilon'^*\mu - \left[h_{A_2}(w)v^\mu + h_{A_3}(w)v'^\mu\right]\varepsilon^*\cdot v, \\
\langle D(v')|A^\mu|\bar{B}^*(v,\varepsilon)\rangle &= h_{\bar{A}_1}(w)(w+1)\varepsilon^\mu - \left[h_{\bar{A}_2}(w)v'^\mu + h_{\bar{A}_3}(w)v^\mu\right]\varepsilon\cdot v', \\
\langle D^*(v',\varepsilon')|A^\mu|\bar{B}^*(v,\varepsilon)\rangle &= i\epsilon^{\mu\nu\alpha\beta}\left\{\left[h_7(w)(v+v')^\mu + h_8(w)(v-v')^\mu\right]\varepsilon_\alpha\varepsilon'_\beta\right. \\
&\quad \left.+ \left[h_9(w)\varepsilon'^*\cdot v\varepsilon_\nu + h_{10}(w)\varepsilon\cdot v'\varepsilon'^*\right]v'_\alpha v_\beta\right\}, \tag{A.2}
\end{aligned}$$

for the axial-vector current. Here,  $\varepsilon^{(l)}$  denote the polarization of the vector mesons. For our purposes, it is convenient to introduce a new set of form factors defined as linear combinations of the functions  $h_i(w)$ . We introduce these form factors in such a way that they reduce to the Isgur–Wise function in the heavy-quark limit, have definite spin–parity quantum numbers, and “diagonalize” the unitarity relations derived in Section 2. Thus, we define the scalar ( $J^P = 0^+$ ) functions (dropping the argument  $w$  for brevity)

$$\begin{aligned}
S_1^{(BD)} &= h_+ - \frac{1+r}{1-r}\frac{w-1}{w+1}h_-, \\
S_2^{(B^*D^*)} &= h_1 - \frac{1+r}{1-r}\frac{w-1}{w+1}h_2, \\
S_3^{(B^*D^*)} &= w\left(h_1 - \frac{1+r}{1-r}\frac{w-1}{w+1}h_2\right) \\
&\quad + \frac{w-1}{1-r}\left[rh_3 - h_4 + (1-wr)h_5 + (w-r)h_6\right], \tag{A.3}
\end{aligned}$$

the pseudoscalar ( $J^P = 0^-$ ) functions

$$\begin{aligned}
P_1^{(BD^*)} &= \frac{1}{1+r} \left[ (w+1) h_{A_1} - (1-wr) h_{A_2} - (w-r) h_{A_3} \right], \\
P_2^{(B^*D)} &= \frac{1}{1+r} \left[ r(w+1) h_{\bar{A}_1} - (r-w) h_{\bar{A}_2} - (rw-1) h_{\bar{A}_3} \right], \\
P_3^{(B^*D^*)} &= h_7 - \frac{1-r}{1+r} h_8,
\end{aligned} \tag{A.4}$$

the vector ( $J^P = 1^-$ ) functions

$$\begin{aligned}
V_1^{(BD)} &= h_+ - \frac{1-r}{1+r} h_-, \\
V_2^{(B^*D^*)} &= h_1 - \frac{1-r}{1+r} h_2, \\
V_3^{(B^*D^*)} &= w \left( h_1 - \frac{1-r}{1+r} h_2 \right) \\
&\quad + \frac{1}{1+r} \left[ (1-wr) h_3 + (r-w) h_4 + (w^2-1) (rh_5 + h_6) \right], \\
V_4^{(BD^*)} &= h_V, \\
V_5^{(B^*D)} &= h_{\bar{V}}, \\
V_6^{(B^*D^*)} &= h_3, \\
V_7^{(B^*D^*)} &= h_4,
\end{aligned} \tag{A.5}$$

and the axial-vector ( $J^P = 1^+$ ) functions

$$\begin{aligned}
A_1^{(BD^*)} &= h_{A_1}, \\
A_2^{(B^*D)} &= h_{\bar{A}_1}, \\
A_3^{(B^*D^*)} &= h_7 - \frac{w-1}{w+1} h_8 + (w-1) h_{10}, \\
A_4^{(B^*D^*)} &= h_7 + \frac{w-1}{w+1} h_8 + (w-1) h_9, \\
A_5^{(BD^*)} &= \frac{1}{1-r} \left[ (w-r) h_{A_1} - (w-1) (rh_{A_2} + h_{A_3}) \right], \\
A_6^{(B^*D)} &= \frac{1}{1-r} \left[ (1-wr) h_{\bar{A}_1} + (w-1) (h_{\bar{A}_2} + rh_{\bar{A}_3}) \right], \\
A_7^{(B^*D^*)} &= h_7 - \frac{1+r}{1-r} \frac{w-1}{w+1} h_8.
\end{aligned} \tag{A.6}$$

In these equations,  $r = m_{D^{(*)}}/m_{B^{(*)}}$  denotes the appropriate ratio of meson masses. The functions  $h_{\bar{V}}$  and  $h_{\bar{A}_i}$ , which have not been defined in Ref. [5], are obtained from the corresponding functions  $h_V$  and  $h_{A_i}$  by an interchange of the heavy-quark masses,  $m_c \leftrightarrow m_b$ .

Luke's theorem protects the functions  $h_+$ ,  $h_{A_1}$ ,  $h_{\bar{A}_1}$ ,  $h_1$ , and  $h_7$  from receiving first-order power corrections at zero recoil [4]. Up to corrections of order  $1/m_Q^2$ , they obey the normalization conditions

$$S_j(1) = \eta_V, \quad A_j(1) = \eta_A, \quad (\text{A.7})$$

where  $\eta_V$  and  $\eta_A$  are the QCD renormalization constants of the vector and axial currents at zero recoil [3]. This implies that, to order  $1/m_Q$ , the functions appearing in the unitarity inequalities for the spin-parity channels  $0^+$  and  $1^+$  in (5) have the same normalization.

In the heavy-quark limit,  $h_+ = h_V = h_{A_1} = h_{A_3} = h_{\bar{V}} = h_{\bar{A}_1} = h_{\bar{A}_3} = h_1 = h_3 = h_4 = h_7 = \xi$ , where  $\xi(w)$  is the universal Isgur-Wise function, while all other functions  $h_i$  vanish. The leading short-distance corrections to this limit can be parametrized in terms of the Wilson coefficients  $C_i$  and  $C_i^5$  of the vector and axial currents ( $i = 1, 2, 3$ ), which are calculable functions of the variable  $w$  and the heavy-quark masses,  $m_b$  and  $m_c$ . For our purposes, it is sufficient to work with the exact one-loop expressions for these functions [39]–[41]. Leading logarithms, which have been summed to all orders in perturbation theory, are universal and cancel in the form-factor ratios we are interested in. In fact, for the same reason we are free to divide out  $C_1$  as a common factor. Then the resulting one-loop expressions are

$$\begin{aligned} \frac{C_1^5}{C_1} &= 1 - \frac{4\alpha_s}{3\pi} r(w), \\ \frac{C_2^{(5)}}{C_1} &= -\frac{2\alpha_s}{3\pi} H_{(5)}(w, 1/z), \\ \frac{C_3^{(5)}}{C_1} &= \mp \frac{2\alpha_s}{3\pi} H_{(5)}(w, z), \end{aligned} \quad (\text{A.8})$$

where  $z = m_c/m_b$ , and

$$\begin{aligned} r(w) &= \frac{1}{\sqrt{w^2 - 1}} \ln \left( w + \sqrt{w^2 - 1} \right), \\ H_{(5)}(w, z) &= \frac{z(1 - \ln z \mp z)}{1 - 2wz + z^2} + \frac{z}{(1 - 2wz + z^2)^2} \left\{ 2(w \mp 1)z(1 \pm z) \ln z \right. \\ &\quad \left. - \left[ (w \pm 1) - 2w(2w \pm 1)z + (5w \pm 2w^2 \mp 1)z^2 - 2z^3 \right] r(w) \right\}. \end{aligned} \quad (\text{A.9})$$

The upper signs refer to the function  $H$ , the lower ones to  $H_5$ .

Similarly, the leading power corrections can be parametrized by six functions  $L_i(w)$  introduced in Ref. [5], which are related to the subleading Isgur–Wise functions  $\eta(w)$  and  $\chi_i(w)$  defined in Ref. [4]. Once again, since we are only interested in form-factor ratios, we can omit the contribution of  $\chi_1(w)$ , which is the same for all meson form factors. Then the resulting expressions are

$$\begin{aligned}
L_1 &= -4(w-1) \frac{\chi_2}{\xi} + 12 \frac{\chi_3}{\xi} \approx 0.72(w-1)\bar{\Lambda}, \\
L_2 &= -4 \frac{\chi_3}{\xi} \approx -0.16(w-1)\bar{\Lambda}, \\
L_3 &= 4 \frac{\chi_2}{\xi} \approx -0.24\bar{\Lambda}, \\
L_4 &= (2\eta-1) \bar{\Lambda} \approx 0.24\bar{\Lambda}, \\
L_5 &= -\bar{\Lambda}, \\
L_6 &= -\frac{2}{w+1} (\eta+1) \bar{\Lambda} \approx -\frac{3.24}{w+1} \bar{\Lambda},
\end{aligned} \tag{A.10}$$

where  $\bar{\Lambda} = m_M - m_Q \approx 0.5 \text{ GeV}$  is the “binding energy” of a heavy meson, and on the right-hand side we have used approximate expressions for the subleading Isgur–Wise functions obtained using QCD sum rules [42].

The corresponding expressions for the functions  $h_i$  are

$$\begin{aligned}
\frac{h_+}{\xi} &= C_1 + \frac{w+1}{2} (C_2 + C_3) + (\varepsilon_c + \varepsilon_b) L_1, \\
\frac{h_-}{\xi} &= \frac{w+1}{2} (C_2 - C_3) + (\varepsilon_c - \varepsilon_b) L_4, \\
\frac{h_V}{\xi} &= C_1 + \varepsilon_c (L_2 - L_5) + \varepsilon_b (L_1 - L_4), \\
\frac{h_{A_1}}{\xi} &= C_1^5 + \varepsilon_c \left( L_2 - \frac{w-1}{w+1} L_5 \right) + \varepsilon_b \left( L_1 - \frac{w-1}{w+1} L_4 \right), \\
\frac{h_{A_2}}{\xi} &= C_2^5 + \varepsilon_c (L_3 + L_6), \\
\frac{h_{A_3}}{\xi} &= C_1^5 + C_3^5 + \varepsilon_c (L_2 - L_3 - L_5 + L_6) + \varepsilon_b (L_1 - L_4), \\
\frac{h_{\bar{V}}}{\xi} &= C_1 + \varepsilon_c (L_1 - L_4) + \varepsilon_b (L_2 - L_5), \\
\frac{h_{\bar{A}_1}}{\xi} &= C_1^5 + \varepsilon_c \left( L_1 - \frac{w-1}{w+1} L_4 \right) + \varepsilon_b \left( L_2 - \frac{w-1}{w+1} L_5 \right),
\end{aligned}$$

$$\begin{aligned}
\frac{h_{\bar{A}_2}}{\xi} &= -C_3^5 + \varepsilon_b (L_3 + L_6), \\
\frac{h_{\bar{A}_3}}{\xi} &= C_1^5 - C_2^5 + \varepsilon_c (L_1 - L_4) + \varepsilon_b (L_2 - L_3 - L_5 + L_6), \\
\frac{h_1}{\xi} &= C_1 + \frac{w+1}{2} (C_2 + C_3) + (\varepsilon_c + \varepsilon_b) L_2, \\
\frac{h_2}{\xi} &= \frac{w+1}{2} (C_2 - C_3) + (\varepsilon_c - \varepsilon_b) L_5, \\
\frac{h_3}{\xi} &= C_1 + \varepsilon_c [L_2 + (w-1) L_3 + L_5 - (w+1) L_6] + \varepsilon_b (L_2 - L_5), \\
\frac{h_4}{\xi} &= C_1 + \varepsilon_c (L_2 - L_5) + \varepsilon_b [L_2 + (w-1) L_3 + L_5 - (w+1) L_6], \\
\frac{h_5}{\xi} &= -C_2 + \varepsilon_c (L_3 - L_6), \\
\frac{h_6}{\xi} &= -C_3 + \varepsilon_b (L_3 - L_6), \\
\frac{h_7}{\xi} &= C_1^5 + \frac{w-1}{2} (C_2^5 - C_3^5) + (\varepsilon_c + \varepsilon_b) L_2, \\
\frac{h_8}{\xi} &= \frac{w+1}{2} (C_2^5 + C_3^5) + (\varepsilon_c - \varepsilon_b) L_5, \\
\frac{h_9}{\xi} &= -C_2^5 + \varepsilon_c (L_3 - L_6), \\
\frac{h_{10}}{\xi} &= C_3^5 + \varepsilon_b (L_3 - L_6), \tag{A.11}
\end{aligned}$$

where  $\varepsilon_b = 1/2m_b$  and  $\varepsilon_c = 1/2m_c$ . Given these explicit expressions, it is straightforward to evaluate the form-factor ratios defined in (24) including the leading corrections to the heavy-quark limit. In order to be consistent, we expand the expressions for the ratios to linear order in  $\alpha_s$  and  $1/m_Q$ . In Table A.1, we show the results for the expansion coefficients in (24), with  $w_0 = 1$ . In the numerical analysis, we use  $\alpha_s = \alpha_s(\sqrt{m_b m_c}) = 0.26$ ,  $z = m_c/m_b = 0.29$ , and  $\bar{\Lambda} = 0.48 \text{ GeV}$ . In Table A.2, we give the corresponding values for the same expansion parameters, but at  $w_0 \approx 1.267$ .

Table A.1: *Theoretical predictions for the coefficients in the expansion of the form-factor ratios  $R_j(w)$  around  $w_0 = 1$*

$F_j$	$A_j$	$B_j$	$C_j$	$D_j$
$S_1$	1.0036	-0.0068	0.0017	-0.0013
$S_2$	1.0036	-0.0355	-0.0813	0.0402
$S_3$	1.0036	0.0776	-0.1644	0.0817
$P_1$	1.1548	-0.2088	0.0032	-0.0009
$P_2$	0.9060	-0.0727	0.0031	-0.0008
$P_3$	1.0325	-0.2116	0.0032	-0.0009
$V_1$	1	0	0	0
$V_2$	1.0681	-0.1944	0.0000	0.0000
$V_3$	1.1361	-0.2474	0.0000	0.0000
$V_4$	1.2179	-0.1428	-0.0015	0.0004
$V_5$	1.0676	-0.0362	-0.0015	0.0004
$V_6$	1.4919	-0.2278	-0.0015	0.0004
$V_7$	1.3416	-0.1987	-0.0015	0.0004
$A_1$	0.9484	-0.0265	-0.0560	0.0266
$A_2$	0.9484	0.0050	-0.0184	0.0078
$A_3$	0.9484	-0.0205	-0.0869	0.0421
$A_4$	0.9484	0.0256	-0.1245	0.0609
$A_5$	0.9484	0.2984	-0.2391	0.1180
$A_6$	0.9484	-0.1699	0.0621	-0.0324
$A_7$	0.9484	-0.0113	-0.0857	0.0414

Table A.2: *Theoretical predictions for the coefficients in the expansion of some of the form-factor ratios  $R_j(w)$  around  $w_0 \approx 1.267$*

$F_j$	$A_j$	$B_j$	$C_j$
$S_1$	1.0018	-0.0061	0.0009
$S_2$	0.9883	-0.0727	-0.0554
$S_3$	1.0140	0.0025	-0.1117
$P_1$	1.0974	-0.2072	0.0026
$P_2$	0.8862	-0.0711	0.0025
$P_3$	0.9743	-0.2100	0.0025
$A_1$	0.9373	-0.0522	-0.0387

## References

- [1] M. Neubert, Phys. Lett. B **264**, 455 (1991); **338**, 84 (1994).
- [2] N. Isgur and M.B. Wise, Phys. Lett. B **232**, 113 (1989); **237**, 527 (1990).
- [3] For a review, see: M. Neubert, Phys. Rep. **245**, 259 (1994); Int. J. Mod. Phys. A **11**, 4173 (1996).
- [4] M.E. Luke, Phys. Lett. B **252**, 447 (1990).
- [5] A.F. Falk and M. Neubert, Phys. Rev. D **47**, 2965 and 2982 (1993).
- [6] M. Shifman, N.G. Uraltsev and A. Vainshtein, Phys. Rev. D **51**, 2217 (1995).
- [7] A. Czarnecki, Phys. Rev. Lett. **76**, 4124 (1996).
- [8] Z. Ligeti, Y. Nir and M. Neubert, Phys. Rev. D **49**, 1302 (1994).
- [9] N.N. Meiman, Sov. Phys. JETP **17**, 830 (1963).
- [10] S. Okubo, Phys. Rev. D **3**, 2807 (1971);  
S. Okubo and I. Shih, Phys. Rev. D **4**, 2020 (1971).
- [11] V. Singh and A.K. Raina, Forts. der Physik **27**, 561 (1979).
- [12] C. Bourrely, B. Machet and E. de Rafael, Nucl. Phys. B **189**, 157 (1981).
- [13] E. de Rafael and J. Taron, Phys. Lett. B **282**, 215 (1992).
- [14] E. de Rafael and J. Taron, Phys. Rev. D **50**, 373 (1994).

- [15] I. Caprini, Z. Phys. C **61**, 651 (1994).
- [16] I. Caprini, Phys. Lett. B **339**, 187 (1994); Phys. Rev. D **52**, 6349 (1995).
- [17] C.G. Boyd, B. Grinstein and R.F. Lebed, Phys. Lett. B **353**, 306 (1995); Nucl. Phys. B **461**, 493 (1996).
- [18] I. Caprini and C. Macesanu, Phys. Rev. D **54**, 5686 (1996).
- [19] I. Caprini and M. Neubert, Phys. Lett. B **380**, 376 (1996).
- [20] C.G. Boyd, B. Grinstein and R.F. Lebed, Phys. Rev. D **56**, 6895 (1997).
- [21] E.J. Eichten and F. Feinberg, Phys. Rev. D **23**, 2724 (1981);  
E.J. Eichten and C. Quigg, Phys. Rev. D **49**, 5845 (1994).
- [22] D.J. Broadhurst, Phys. Lett. B **101**, 423 (1981).
- [23] S.C. Generalis, J. Phys. G **16**, 367 and 785 (1990).
- [24] A. Djouadi and P. Gambino, Phys. Rev. D **49**, 3499 (1994).
- [25] L.J. Reinders, S. Yazaki and H.R. Rubinstein, Phys. Rep. **127**, 1 (1985).
- [26] I. Caprini, J. Phys. A: Math. Gen. **14**, 1271 (1981);  
I. Caprini, I. Guiasu and E.E. Radescu, Phys. Rev. D **25**, 1808 (1982).
- [27] J.L. Walsh, *Interpolation and Approximation by Rational Functions in the Complex Domain* (American Mathematical Society, Providence, RI, 1956).
- [28] R.E. Cutkoski and B.B. Deo, Phys. Rev. **174**, 1859 (1968).
- [29] Z. Nehari, *Conformal Mapping* (Dover Publ., 1952).
- [30] C.G. Boyd and R.F. Lebed, Nucl. Phys. B **485**, 275 (1997).
- [31] C.G. Boyd, Z. Ligeti, I.Z. Rothstein and M.B. Wise, Phys. Rev. D **55**, 3027 (1997).
- [32] CLEO Collaboration (J.E. Duboscq et al.), Phys. Rev. Lett. **76**, 3898 (1996);  
CLEO Collaboration (A. Anastassov et al.), Preprint CLEO CONF 96-8, ICHEP96 PA05-079, contributed paper to the 28th International Conference on High Energy Physics, Warsaw, Poland, July 1996.
- [33] For a discussion of this uncertainty, see: L.K. Gibbons, Proceedings of the 28th International Conference on High-energy Physics (ICHEP 96), Warsaw, Poland, July 1996, p. 183 [hep-ex/9704017].
- [34] CLEO Collaboration (B. Barish et al.), Phys. Rev. D **51**, 1014 (1995).



- [35] ARGUS Collaboration (H. Albrecht et al.), Z. Phys. C **57**, 533 (1993); Phys. Rep. **276**, 223 (1996).
- [36] ALEPH Collaboration (D. Buskulic et al.), Phys. Lett. B **395**, 373 (1997).
- [37] DELPHI Collaboration (P. Abreu et al.), Z. Phys. C **71**, 539 (1996).
- [38] OPAL Collaboration (K. Ackerstaff et al.), Phys. Lett. B **395**, 128 (1997).
- [39] J.E. Paschalis and G.J. Gounaris, Nucl. Phys. B **222**, 473 (1983);  
F.E. Close, G.J. Gounaris and J.E. Paschalis, Phys. Lett. B **149**, 209 (1984).
- [40] A.F. Falk and B. Grinstein, Phys. Lett. B **249**, 314 (1990).
- [41] M. Neubert, Phys. Rev. D **46**, 2212 (1992); Nucl. Phys. B **371**, 149 (1992).
- [42] M. Neubert, Z. Ligeti and Y. Nir, Phys. Lett. B **301**, 101 (1993); Phys. Rev. D **47**, 5060 (1993);  
Z. Ligeti, Y. Nir and M. Neubert, Phys. Rev. D **49**, 1302 (1994).